Materials Letters 132 (2014) 327–330

Contents lists available at ScienceDirect

Materials Letters

journal homepage: www.elsevier.com/locate/matlet

Structural, magnetic and optical properties of Ho–Co codoped $BiFeO_3$ nanoparticles

Manisha Arora, Prakash Chandra Sati, Sunil Chauhan, Manoj Kumar*, Sandeep Chhoker

Department of Physics and Materials Science and Engineering, Jaypee Institute of Information Technology, Noida-201307, India

ARTICLE INFO

Article history:
Received 25 April 2014
Accepted 17 June 2014
Available online 24 June 2014

Keywords:
Multiferroics
Sol gel
Magnetic properties
Optical properties

ABSTRACT

Structural, magnetic and optical properties of $Bi_{0.85}Ho_{0.15}Fe_{1-x}Co_xO_3$ ($x=0.0–0.15$) nanoparticles have been studied. X-ray diffraction patterns and Raman spectra demonstrate orthorhombic structure for all samples. Spontaneous magnetization of Ho–Co co-substituted $BiFeO_3$ nanoparticles increased up to 3.71 emu/g for $x=0.15$. Electron spin resonance analysis showed that the addition of Co^{2+} ions is likely to increase the spin canting angle and reduces anisotropy which favors the enhanced ferromagnetism. Optical studies in the spectral range from 1.1 to 5 eV showed two d–d crystal field transitions and three charge–transfer transitions with band gap variation from 2.60 to 2.38 eV.

1. Introduction

Multiferroic materials with two or more coexisting order parameters have created great scientific and industrial interest. These materials provide a wide range of potential applications in information storage process, spintronics, and multi-state memories due to the possible interaction between order parameters [1,2]. Among all, $BiFeO_3$ (BFO) occupies a special place as it exhibits ferroelectric (Curie temperature $T_c \sim 1103$ K) and G-type antiferromagnetic (Neel temperature $T_N \sim 643$ K) properties at room temperature [3,4]. The crystal structure of BFO is described by the rhombohedral structure of space group *R*3*c*. BFO is very capable for the practical applications, however, the presence of G-type antiferromagnetic ordering with cycloidal spin structure of wavelength of 62 nm in bulk BFO does not permit the observation of any net magnetization. The existence of oxygen vacancies caused by the presence of Fe^{2+} ions and volatilization of Bi^{3+} ions leads to high leakage current which hinders the practical application of BFO [4,6]. In order to improve the magnetic as well as electric properties, co-substitution with La/Mn, Er/Co, Eu/Co and Ba/Co ions has been carried out [3–6]. Single phase $Bi_{0.85}Ho_{0.15}Fe_{1-x}Co_xO_3$ ($x=0.0–0.15$) nanoparticles were prepared by a tartaric acid modified the sol–gel method and their structures, surface morphology, magnetic and optical properties were studied.

2. Experimental

The nanoparticles of $Bi_{0.85}Ho_{0.15}Fe_{1-x}Co_xO_3$ ($x=0.0–0.15$) were synthesized by a sol–gel method. The details of synthesis process are described elsewhere [4]. The powder X-ray diffraction (XRD) of the samples was carried out using Brucker D8 Advance. Raman measurement was done using Renishaw Raman spectrometer. Magnetic studies were performed on VSM (Lakeshore VSM 7410) and ESR spectra were recorded on (Bruker EMX spectrometer). A UV–visible diffuse reflectance spectrum (Ocean optics UV–visible 4000) was used for optical study.

3. Results and discussion

Fig. 1(a) shows the Rietveld refined XRD patterns of $Bi_{0.85}Ho_{0.15}Fe_{1-x}Co_xO_3$ ($x=0.0–0.15$) samples. The XRD patterns confirmed single phase formation for all the samples. All the observed lines for each sample could be indexed to an orthorhombic phase with space group *Pnma* unlike pure BFO which possesses rhombohedral with space group *R*3*c* [7]. This type of structure has already been reported in codoped BFO nanoparticle [4,8]. The XRD patterns have tendency of shifting the peaks towards lower angles with increasing Co^{2+} ions concentration which may be related to the fact that larger Co^{2+} (0.79 Å) ions have entered at smaller Fe^{3+} (0.645 Å) ions site in BFO lattice. The orthorhombic structure in these samples may be ascribed to the structural distortion due to ionic radii mismatch between the dopant ions and the parent ions of BFO lattice.

Fig. 1(b)–(e) shows the typical TEM images of the samples. It is evident from these images that the nanoparticles are agglomerated and irregular in shape. The average particle size is less than 50 nm for

---

* Corresponding author.
E-mail address: manoj.chauhan@jiit.ac.in (M. Kumar).

http://dx.doi.org/10.1016/j.matlet.2014.06.110
0167-577X/

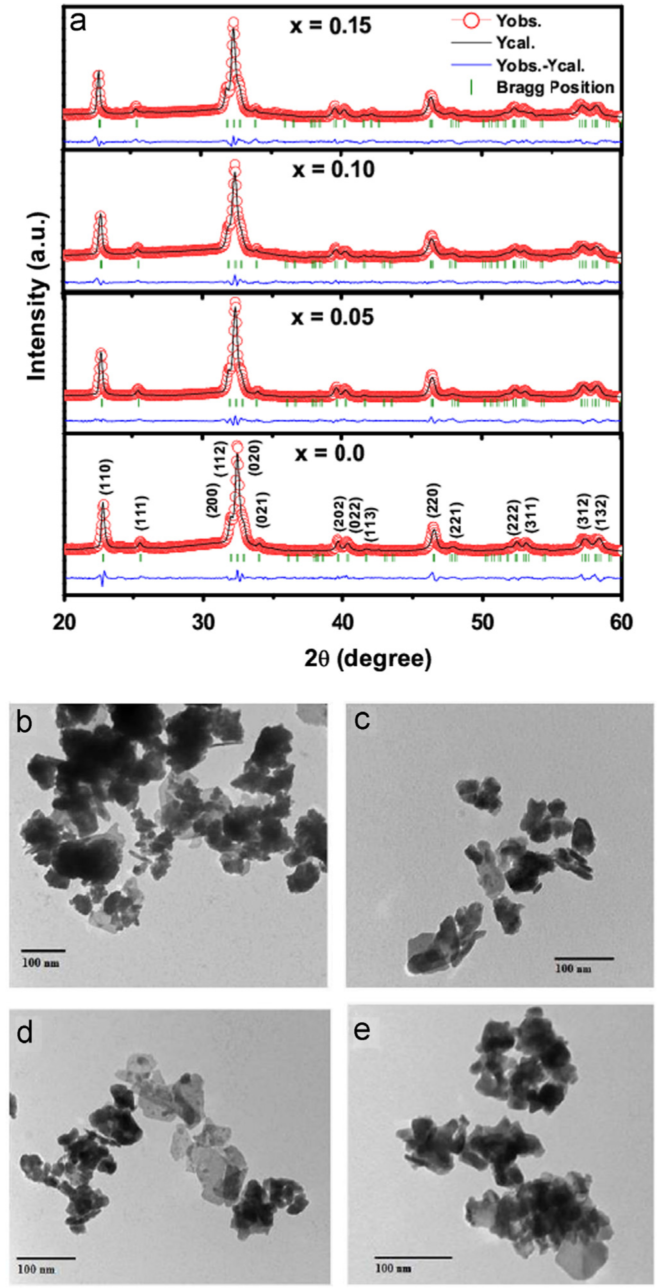

Fig. 1. (a) Rietveld refined XRD patterns for $Bi_{0.85}Ho_{0.15}Fe_{1-x}Co_xO_3$ nanoparticles. TEM images for (b) $x=0.0$, (c) $x=0.05$, (d) $x=0.10$ and (e) $x=0.15$ samples.

$x=0.0$ sample which further decreases with increasing Co^{2+} substation on Fe site.

Fig. 2(a) shows Raman spectroscopy results for $Bi_{0.85}Ho_{0.15}Fe_{1-x}Co_xO_3$ ($x=0.0$–0.15) samples at room temperature and Fig. 2 (b) represents the deconvoluted Raman active modes for $x=0.0$ sample. According to group theory the Raman active modes of rhombohedral structure of BFO can be summarized using the irreducible representation: $\Gamma_{\text{Raman}}=4A_1+9E$ [9]. Each Raman active phonon mode can be identified and comparison of the observed Raman modes for $x=0.0$ sample with the standard Raman spectra of pure BFO showed that modes shift towards higher wave number side indicate the distortion in crystal structure [7,9]. The substitution of Co ions results in intensity reduction of A_1-2 and E-6 modes. However, E-9 mode shifts towards lower wave number side with increasing x. The E-9 mode is assigned to $Fe–O_2$ bonding which is related with the octahedral rotation critical to weak magnetism [10]. Moreover, an enhanced Raman active mode ($\sim 470\ cm^{-1}$) mainly related to the oxygen associated vibration, appeared in all codoped samples indicating the increase in oxygen vacancies with increasing x [11]. The unidentified E mode observed at $105\ cm^{-1}$ may be associated with the conversion between A and E modes [11].

Fig. 2(c) displays the absorption spectrum for $Bi_{0.85}Ho_{0.15}Fe_{1-x}Co_xO_3$ ($x=0.0$–0.15) samples. Ramirez et al. reported that six d to d transitions are expected between 0 and 3 eV by considering the C_{3v} local symmetry of Fe^{3+} ions in BFO lattice and using the correlation group and subgroup analysis for the symmetry breaking. Two weak bands below 2 eV centered at 1.3 eV ($^6A_{1g}\rightarrow {}^4T_{1g}$) and 1.75 eV ($^6A_{1g}\rightarrow {}^4T_{2g}$) are assigned as on-site d–d crystal field transitions of Fe^{3+} ions [12]. A weak band $\sim$2.5 eV superimposed on the tail of strong band $\sim$3 eV is assigned to dipole-forbidden p–d C–T transition. Two intense bands $\sim$3 and 4.3 eV are attributed to dipole allowed p–d CT transitions in FeO_6 octahedral [13]. A small shift in d–d and C–T transition bands clearly indicates that codoping increases the internal chemical pressure as a result of change in FeO_6 octahedral unit cell. The direct band gap of the samples were extracted via a linear extrapolation of $(\alpha E)^2$ versus E plots to zero as shown in Fig. 2(d). The values of band gap were found to be 2.60, 2.54, 2.41 and 2.38 eV for $x=0.0$, 0.05, 0.10 and 0.15 samples respectively.

Magnetization–magnetic field (M–H) hysteresis loops for $Bi_{0.85}Ho_{0.15}Fe_{1-x}Co_xO_3$ ($x=0.0$–0.15) samples are shown in Fig. 3 (a). All the samples exhibit weak ferromagnetic behavior which further improved with increasing Co^{2+} ions concentration. The value of spontaneous magnetization increases significantly from 1.2 emu/g for $x=0.0$ to 3.73 emu/g for $x=0.15$ which is larger than the earlier reported values for codoped BFO [4–6]. Multiple factors are responsible for ferromagnetic behaviour in codoped BFO, such as particle size of codoped BFO nanoparticles are below 62 nm (smaller than the period length of cycloid spin structure of BFO). Modification in cycloid spin structure gives rise to ferromagnetic ordering instead of antiferromagnetic ordering because with the reduction of particle size surface to volume ratio became very large which gives rise to uncompensated spins at the particle surface and these uncompensated spins contribute to the arising of net magnetization. The enhancement in magnetization may be attributed to increase in double exchange interaction of Fe^{3+}–O–Fe^{2+} due to increasing Co^{2+} ions in BFO lattice. In addition, substitution of Co^{2+} ions with a different valence and atom radius for Fe^{+} ions in some atom positions, the balance between the two adjacent antiparallel spin lattices of Fe^{3+} is broken. The ferromagnetic coupling via oxygen is favored due to the formation of Fe–O–Co chains, which contributes to enhancement of magnetization.

ESR spectra of the codoped samples at RT are shown in Fig. 3 (b). Only one signal with asymmetric line shape was obtained for each sample and ESR lines shifts to the left (higher g values). The g-values can be calculated by using the relation: $h\nu=g\mu_B H_r$, where h is Planck's constant, ν is operating frequency, μ_B is Bohr Magnetron and H_r is resonance field. All the g-values were greater than 2, demonstrating the ferromagnetic character of the samples [14]. The asymmetry parameter P_{asy} is defined as: $P_{asy}=(1-h_U/h_L)$, where h_U is the height of the absorption peak above the base line and h_L is the height of the absorption peak below the base line of the ESR spectra. The magnetocrystalline anisotropy reduces with the incorporation of Co^{2+} ions, hence provides low energy to stabilize the crystal structure and the formation of cycloid is not favored. The line width of the signal (ΔH_{p-p}) was calculated from the peak-to peak distance on the axis of applied field H. Degree of spin canting is directly related to g-values through the vector coefficient D by the relation: $D\approx(\Delta g/g)$